Guiding of laser pulses in plasma channels created by the ignitor-heater technique

Cite as: Physics of Plasmas **6**, 2269 (1999); https://doi.org/10.1063/1.873503
Submitted: 18 November 1998 . Accepted: 17 February 1999 . Published Online: 26 April 1999

P. Volfbeyn, E. Esarey, and W. P. Leemans

Guiding of laser pulses in plasma channels created by the ignitor-heater technique*

P. Volfbeyn,† E. Esarey, and W. P. Leemans
Center for Beam Physics, Ernest Orlando Lawrence Berkeley National Laboratory, University of California, Berkeley, California 94720

(Received 18 November 1998; accepted 17 February 1999)

Experimental and theoretical investigations of laser guiding in plasma channels are reported. Intense ($<5\times10^{17}$ W/cm^2), short (75 fs) laser pulses have been injected and guided in channels produced using a novel ignitor-heater technique, which uses two laser pulses. The ignitor, an ultrashort (<100 fs) laser pulse, is brought to a line focus to ionize the gas jet. The heater pulse (160 ps long) is subsequently used to heat the existing spark via inverse Bremsstrahlung. The hydrodynamic shock expansion creates a channel. This technique allows the creation of slab or cylindrical channels in low atomic number gases, e.g., hydrogen. The channel profile was diagnosed with time resolved longitudinal interferometry. The effects of laser beam size and divergence mismatch at the channel entrance and leakage of the laser energy out of the channel are studied theoretically and experimentally in one and two transverse dimensions. An all-optical channel wake diagnostic based on Fourier domain interferometry is discussed, and a holographic-type inversion technique is proposed to increase the accuracy and reach of this method. [S1070-664X(99)97205-1]

I. INTRODUCTION

Optical guiding of intense laser pulses in plasma channels[1] is beneficial to a variety of applications, including plasma-based accelerators,[2] harmonics generation,[3] x-ray lasers,[4] and advanced laser-fusion schemes.[5] Laser propagation is typically limited by diffraction, the characteristic distance of which in vacuum is the Rayleigh length $Z_R=\pi r_0^2/\lambda$, where r_0 is the laser spot radius at focus of a Gaussian laser mode with an intensity profile $I\propto\exp(-2r^2/r_0^2)$, $\lambda=2\pi c/\omega_0$ is the laser wavelength, and ω_0 is the laser frequency. For example, in the laser wakefield accelerator,[2] plasma wave excitation requires laser intensities on the order of 10^{18} W/cm^2, which implies μm-scale spot sizes for terawatt (TW)-level laser powers ($Z_R\simeq300\,\mu$m for $r_0=10\,\mu$m and $\lambda=1\,\mu$m). Hence, high electron energy gains require guiding over long acceleration distances (many Z_R).

Plasma channels have been proposed as a means of guiding laser pulses.[2,6–8] The index of refraction in a plasma of density n is approximately $\eta_R\simeq1-\omega_p^2/2\omega_0^2$, where $\omega_p=(4\pi ne^2/m_e)^{1/2}$ is the electron plasma frequency. As in an optical fiber, a plasma channel can provide optical guiding if the index of refraction peaks on axis, $\partial\eta_R/\partial r<0$, which can be achieved with a plasma density profile that has a local minimum on axis, $\partial n/\partial r>0$. Specifically, a channel with a radially parabolic density profile of the form $n(r)=n_0+\Delta nr^2/r_0^2$ can guide a Gaussian laser pulse with a constant spot size r_0 provided the channel depth Δn satisfies $\Delta n=\Delta n_c$, where $\Delta n_c=1/\pi r_e r_0^2$ is the critical channel depth[6] and $r_e=e^2/m_ec^2$ is the classical electron radius, i.e., $\Delta n_c[\mathrm{cm}^{-3}]\simeq1.13\times10^{20}/r_0^2[\mu\mathrm{m}]$.

Plasma channels have been created in the laboratory by a variety of methods: (i) passing a long laser pulse through an optic to create a line focus in a gas, which ionizes and heats the gas, creating a radially expanding hydrodynamic shock,[7–14] (ii) using a slow capillary discharge to control the plasma profile,[15] and (iii) using the ponderomotive force of an intense, relativistically self-guided laser pulse in a plasma, which creates a channel in its wake.[16–24]

To guide highly intense laser pulses, plasmas channels must be produced in deeply ionized gases, where the density profile cannot be changed by the guided pulse through further ionization. An increase in density on axis would lead to ionization induced refraction[25] and hence negate the guiding. Reaching sufficient depth of ionization is most easily satisfied through the use of low atomic number, Z, gases.

In laser created channels, the use of low Z gases (e.g., hydrogen or helium) requires that the channel producing laser pulse satisfy two conditions: (1) be sufficiently intense to create free electrons through barrier suppression ionization[26] (typically $>2\times10^{14}$ W/cm^2) and (2) be energetic and long (several 100 mJ's/pulse in >100 ps) but relatively low intensity ($<1\times10^{13}$ W/cm^2) to efficiently heat the plasma through inverse Bremsstrahlung heating. Short intense pulses are indeed inefficient at heating plasmas since the collision frequency is reduced for large quiver velocities.[27]

To meet these two conditions, we have developed a novel technique which, rather than utilizing a single laser pulse for ionization and heating, makes use of two laser pulses.[13] A sub-ps low energy but intense ($\gtrsim2\times10^{14}$ W/cm^2) ''ignitor'' pulse is first used to create the initial spark, followed by a long (tens to hundreds of ps), ener-

*Paper Q7I1.2 Bull. Am. Phys. Soc. **43**, 1844 (1998).
†Invited speaker.

getic (>100 mJ) ''heater'' pulse. Using the ignitor-heater method, the total laser energy required to generate a channel with length L_{ch} is greatly reduced compared to a single pulse. As a practical example, to achieve $>2\times10^{14}\,\mathrm{W/cm^2}$ in a 100 ps long pulse, focused to a spot size of $5\,\mu\mathrm{m}\times5\,\mathrm{mm}$ ($L_{ch}=5\,\mathrm{mm}$) would require 5 J laser energy compared to 5 mJ for a 100 fs pulse.

The geometrical shape of the plasma channel cross section is strongly affected by the initial transverse shape of the hot plasma volume. With the ignitor-heater method, control of the initial spark shape is possible by appropriate choice of the propagation geometry of the two pulses. As will be shown, slab-like channels were produced by allowing the ignitor and heater beams to copropagate and cylindrically symmetric channels were created by propagating the two beams orthogonally to each other thereby limiting the hot plasma region to the intersection volume of the two beams.

In practice, the transverse extent and peak plasma density of the channel are finite. Hence, tunneling of the laser radiation through the channel wall becomes an important loss factor.[8] Similar to glass fibers, coupling a laser beam into a plasma fiber is subject to losses from mode mismatch and reflections at the entrance of the fiber. While the mode mismatch losses in the two cases are very similar, the nature of the entrance reflection is more complicated in a plasma channel. A gas jet must be used in an evacuated chamber to avoid ionization induced refraction[25] that would occur in a statically filled experimental chamber. This paper addresses guiding loss mechanisms and beam propagation issues, both theoretically and experimentally, in transversely elongated (slab) channels as well as cylindrically symmetric (round) channels.

Measurement of the wake excited in plasma channels is the next step in the development of a laser wakefield accelerator stage. Longitudinal fs interferometry, using an externally injected laser pulse and measuring the phase shift imparted to it by the plasma wave as a function of delay time after the driving pulse, was shown to be a valuable technique for measuring the wake amplitude in experiments in homogeneous plasmas.[28,29] A new modification of the longitudinal fs interferometry diagnostic method is proposed to enable time resolved measurement of the channel wake.

II. CHANNEL PRODUCTION

The experiments were performed using the multi-TW Ti:Al_2O_3 laser ($\lambda\simeq820\,\mathrm{nm}$) at the l'OASIS laboratory of the Center for Beam Physics at Lawrence Berkeley National Laboratory.[12,13] To implement the ignitor-heater method, two laser pulses were combined in a line focus by means of cylindrical optics onto a gas jet (Fig. 1). A 75 fs, 20–40 mJ intense ignitor pulse was focused to a $\sim5\,\mu\mathrm{m}\times5\,\mathrm{mm}$ area by reflecting off a cylindrical reflector, resulting in an intensity of $\sim5\times10^{14}\,\mathrm{W/cm^2}$. The cylindrical reflector was a plano-concave ($R=38\,\mathrm{mm}$) cylindrical lens, coated with a dielectric high reflection coating for 45° angle of incidence. The use of a reflective optic was required to avoid undesirable nonlinear effects that would prevent obtaining a well focused, near diffraction limited beam spot. The heater pulse

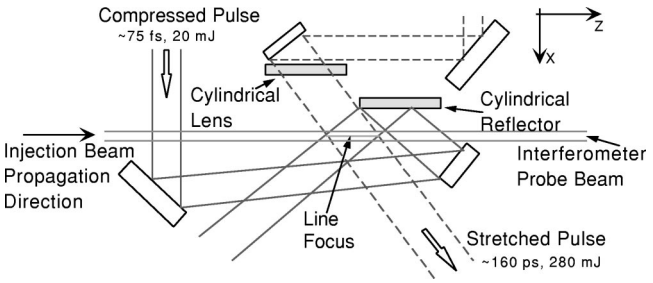

FIG. 1. Experimental Setup.

(~270 mJ, 160 ps long) was focused with an F/5 refractive cylindrical lens (focal length $f_l=50\,\mathrm{mm}$) at the exact location of the ignitor focus. In addition to the ease of the optical setup, stemming from the fact that the channel forming beams propagate perpendicularly to the guided pulse, the use of two independent cylindrical optics provided precise independent adjustment of the angles of incidence and positions of the line foci.

A Mach–Zehnder-type interferometer with a measured spatial resolution of 4 μm was built to measure line integrated plasma density. This interferometer measures the relative spatial phase shift between two blue (410 nm) ~50 fs pulses, one propagating through plasma (down the channel axis, perpendicular to the ignitor-heater pulses) and one through air (see Fig. 1). These pulses were produced by frequency doubling and were synchronized with the high power beams used in the plasma production. The evolution of the transverse plasma density profile was measured with a temporal resolution determined by the duration of the blue pulse.

The ignitor-heater scheme was first implemented with both pulses propagating in the same plane through a nitrogen- or hydrogen-backed gas jet. In this geometry, heat is deposited there where the ignitor pulse intensity exceeds the ionization threshold. Figure 2(a) shows interferograms taken with the interferometer pulse delayed by 560 ps and by 1 ns with respect to the heater pulse in N_2 at 1000 psi. From the inferred plasma density line outs of Fig. 2(b), it is seen that a plasma density depression is created only in the vertical direction. These slab channels provide one-dimensional

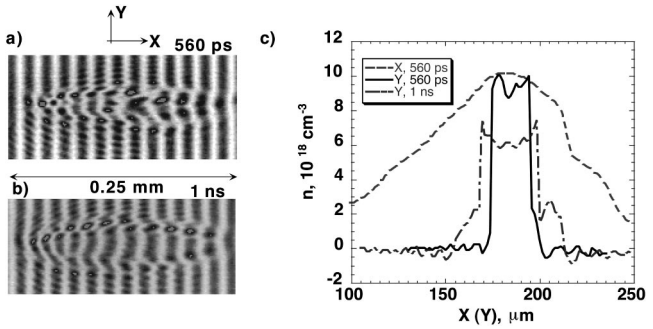

FIG. 2. Channel interferograms at (a) 560 ps and (b) 1 ns after the heater pulse in N_2 at 1000 psi, both ignitor and heater pulses propagate along the x axis, interferometer beam travels along the z axis, the gas jet plume is much wider than the x extent of the channel; (b) inferred plasma density line outs: $n(x)$ (dashed curve) and $n(y)$ (solid curve) at 560 ps; and $n(y)$ (dot-dash curve) at 1 ns.

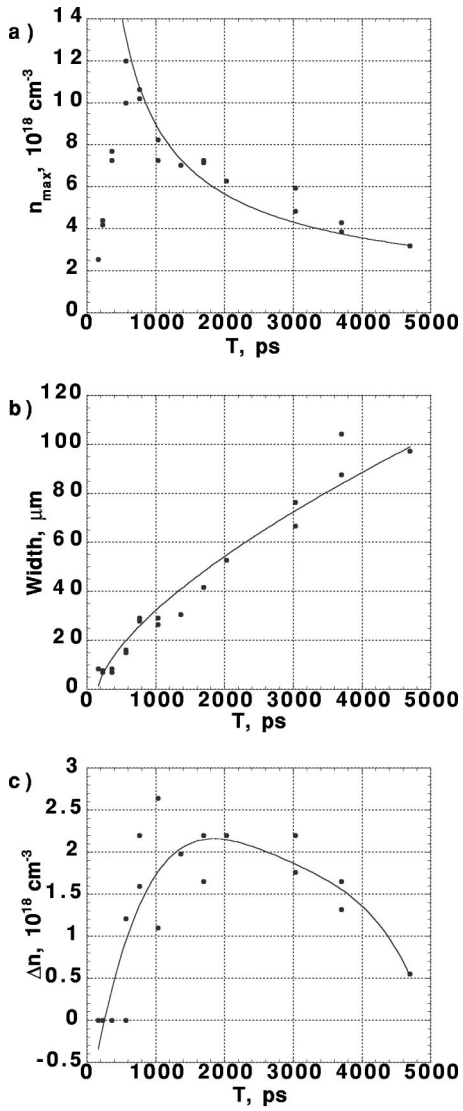

FIG. 3. Channel evolution vs time T after spark ignition in N_2 at 1000 psi: (a) maximum density n_{max} (points are data; curve is a $T^{-2/3}$ fit), (b) distance between n_{max} peaks (points are data; curve is a $T^{2/3}$ fit), and (c) $\Delta n_{ch} = n_{max} - n_0$ (points are data; curve is fourth order polynomial fit).

(1D) guiding. The x size of the channels roughly corresponds to the Rayleigh range of the ignitor pulse. Figure 3 shows, as obtained from interferograms (Fig. 2), the evolution of (a) maximum density n_{max}, (b) distance between density peaks $2x_{ch}$, and (c) $\Delta n_{ch} = n_{max} - n_0$ of the channels, where n_0 is the on-axis density, versus time T after spark ignition in N_2 at 1000 psi. As expected from 1D hydrodynamic shock theory,[13] $x_{ch} \sim T^{2/3}$ and, once plasma production ceases, $n_{max} \sim T^{-2/3}$ (these fits are shown in Fig. 3).

To create cylindrically symmetric channels, the ignitor and heater beams were made to propagate orthogonally to each other (and to the guided beam). This 90° geometry limited the transverse extent of the initial heat deposition volume to the small intersection volume of the two beams (typically 5 μm×5 μm). Figures 4(a) and 4(b) show the geometry for producing slab-like and cylindrically symmetric plasma channels, respectively.

To demonstrate the change in channel shape, shadowgrams were used [Figs. 4(c) and 4(d)]. A shadowgram is obtained by taking an image of the probe interferometric beam (with the reference beam blocked) at the exit of the channel. Refraction in the channel walls expels the blue light, thus casting a shadow on the image of the probe beam. The part of the probe beam that falls inside of the channel walls was observed to be guided. Figures 4(c) and 4(d) clearly demonstrate the effect of the geometry change: the 1D elongated channels of the in-plane configuration [Fig. 4(c)] are contrasted by the round 90° configuration channels [Fig. 4(d)].

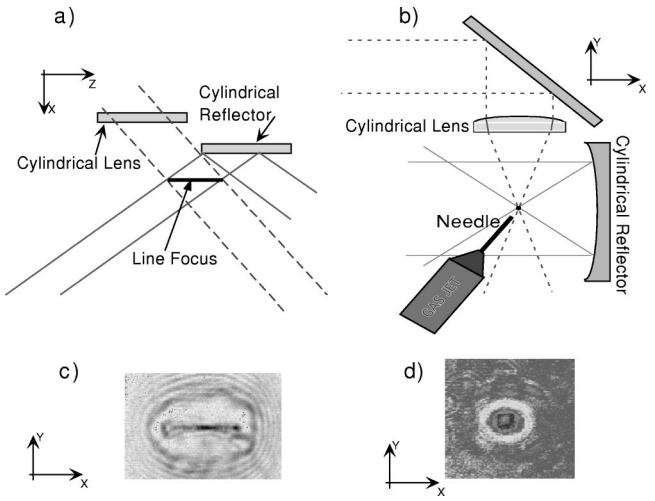

FIG. 4. (a) In-plane laser beam combining and (b) 90° beam configurations; with (c) and (d) the corresponding channel shadowgrams in the x,y plane.

III. THEORY OF FINITE CHANNELS

Experimentally created channels do not have infinitely high walls (i.e., densities). Rather, the channel walls reach a peak height at a finite radius beyond which the density rapidly falls off to zero. In such a channel, the laser modes are ''quasibound'' or ''leaky,'' i.e., the mode can tunnel through the channel wall and couple to the continuum.[8,9] The following analytical calculations assume an idealized form for a finite channel: $n(r) = n_0 + \Delta n r^2/r_0^2$ for $0 < r < r_{ch}$ and $n(r) = 0$ for $r > r_{ch}$, where r_{ch} is the channel radius (an infinite channel corresponds to $r_{ch} = \infty$). The leakage rate depends on channel parameters as well as on the laser mode profile.

If the laser mode is not perfectly matched in the channel, i.e., injected at the channel entrance with an initial spot size $r_{si} \neq r_0$, then the laser spot size r_s will oscillate about its matched value r_0. This is equivalent to exciting higher order modes in the channel. The leakage rate for the higher order modes is much larger than the fundamental, and hence, any power not initially coupled to the low order modes will be rapidly lost from the channel. Before discussing higher-order modes, leakage of the fundamental will be estimated for the 1D slab channel geometry of the experiments discussed in Sec. II.

A. Slab channels

Assuming that the envelope $\hat{E}$ of the laser field $E=\hat{E}(x,z)\exp(ik_z z-i\omega t)$ varies slowly compared to the laser frequency ω and axial wave number k_z, the laser field evolution is described by the paraxial wave equation

$$\left(\nabla_\perp^2+\frac{\omega^2}{c^2}-k_z^2+2ik_z\frac{\partial}{\partial z}\right)\hat{E}=k_p^2\hat{E}, \tag{1}$$

where $k_p^2=k_{p0}^2 n(x)/n_0$, $k_{p0}^2=4\pi e^2 n_0/mc^2$, and $n(x)=n_0+\Delta n x^2/x_0^2$ for $0<x<x_{\rm ch}$ and $n(x)=0$ for $x>x_{\rm ch}$. For an infinite channel, $x_{\rm ch}=\infty$, an exact solution to Eq. (1) is the matched fundamental Gaussian mode $\hat{E}=E_0\exp(-x^2/x_0^2)$, provided $\Delta n=\Delta n_c=1/\pi r_e x_0^2$ and that ω and k_z satisfy the dispersion relation for the bound (guided) mode $\omega^2/c^2-k_z^2=k_{p0}^2+2/x_0^2$.

For a finite channel (finite $x_{\rm ch}$), leakage will occur. Assuming that this leakage rate is small compared to the natural diffraction that would occur in the absence of the channel, tunneling of the quasibound mode can be estimated by neglecting the last term on the left of Eq. (1). Furthermore, the axial wave number k_z will be approximated by its value for a matched bound mode in an infinite channel $k_z\simeq\omega^2/c^2-k_{p0}^2-2/x_0^2$. Hence, $[\partial^2/\partial x^2+K_x^2(x)]\hat{E}=0$, where $K_x^2=2x_0^2-4x^2/x_0^4$. Leakage can be estimated with WKB tunneling theory.[30] In particular, the transverse transmission coefficient $T_\perp$ of the mode through the wall is given by

$$T_\perp\simeq\exp\left(-2\int_{x_{\rm tr}}^{x_{\rm ch}}dx|K_x|\right), \tag{2}$$

where $x_{\rm tr}$ is the turning point defined by $K_x=0$, i.e., $x_{\rm tr}=x_0/\sqrt{2}$. Furthermore, the attenuation of the mode power within the channel is given by $P\simeq P_0\exp(-T_\perp z/Z_p)$, where P_0 is the mode power at $z=0$ and Z_p is the half period of a quasibound ray within the channel

$$Z_p\simeq 2k_z\int_0^{x_{\rm tr}}dx|K_x|^{-1}. \tag{3}$$

For the finite parabolic channel

$$T_\perp\simeq[R_x+(R_x^2-1)^{1/2}]\exp[-R_x(R_x^2-1)^{1/2}] \tag{4}$$

and $Z_p=\pi Z_R$, where $Z_R=(\omega/c)x_0^2/2$ and $R_x=x_{\rm ch}/x_{\rm tr}=\sqrt{2}x_{\rm ch}/x_0$. For an infinite channel, $R_x=\infty$ and $T_\perp=0$, i.e., the mode is completely confined by the channel. For $x_{\rm ch}=x_{\rm tr}$, $T_\perp=1$ and the beam diffracts.

As an example, consider the experiments of Sec. II. The channel shape, 600 ps after ignition, is characterized approximately by an on-axis density $n_0\simeq 8\times10^{18}\,{\rm cm}^{-3}$ with a maximum density $n_{\rm ch}\simeq 1\times10^{19}\,{\rm cm}^{-3}$ at a channel radius $x_{\rm ch}\simeq 8\,\mu$m, i.e., $\Delta n_{\rm ch}=n(x_{\rm ch})-n_0\simeq 2\times10^{18}\,{\rm cm}^{-3}$. For these parameters the matched spot size is $x_0\simeq(x_{\rm ch}^2/\pi r_e\Delta n_{\rm ch})^{1/4}\simeq 7.8\,\mu$m corresponding to a matched Rayleigh length $Z_R\simeq 230\,\mu$m. The transverse transmission coefficient is $T_\perp\simeq 0.53$ and, hence, after $z=1$ mm, the power confined within the channel is $P/P_0\simeq 0.48$. This confinement of $\sim$50% of the guided power over a $\sim$1 mm channel is in good agreement with the data of Sec. IV.

B. Cylindrical channels

The propagation of a low power laser pulse in a finite plasma channel can be analyzed by applying the source dependent expansion (SDE) to the paraxial wave equation.[1,31,32] An envelope equation describing the evolution of the laser spot size $r_s(z)$ can be derived using the following idealized assumptions: (i) the laser field is described by a single SDE Laguerre–Gaussian mode and (ii) coupling to other SDE modes and, consequently, mode leakage from the channel, is neglected. The resulting envelope equation describes the gross behavior of the laser field and delineates under what conditions the bulk of the pulse energy will be initially trapped within the channel. Leakage from the channel can be estimated with WKB tunneling theory. A finite parabolic channel is assumed: $n(r)=n_0+\Delta n r^2/r_0^2$ for $r<r_{\rm ch}$ and $n(r)=0$ for $r>r_{\rm ch}$.

Consider a laser field $E=\hat{E}\exp[ik(z-ct)]+$c.c., where $\omega=ck$ is the laser frequency, $\hat{E}=\hat{E}_{m,p}L_m^p(\chi)\exp[-(1-i\alpha)\chi/2]\cos(p\theta)$, $\hat{E}_{m,p}(z)$ is the complex amplitude, $L_m^p(\chi)$ is a generalized Laguerre polynomial, $\chi=2r^2/r_s^2(z)$, and m and p are the radial and poloidal mode numbers. Under the above assumptions, $r_s(z)$ evolves via

$$\frac{d^2r_s}{dz^2}=\frac{4}{k^2r_s^3}[1+kr_s^2B(z)], \tag{5}$$

$$B=\frac{m!}{2k(m+p+1)!}\int_0^\infty d\chi k_p^2\chi^pL_m^pL_{m+1}^p\exp(-\chi), \tag{6}$$

where $k_p^2(r)=k_{p0}^2n(r)/n_0$. Also, $\alpha=(kr_s/2)\partial r_s/\partial z$ and $\partial(r_s^2|\hat{E}_{m,p}|^2)/\partial z=0$ such that the mode power at each $z-ct$ slice is conserved. For an infinite channel ($r_{\rm ch}=\infty$), $B=B_I=-(\Delta n/\Delta n_c)r_s^2/kr_0^4$ for all m and p.[32] Hence, the condition for guiding any mode with $r_s=r_0$ is $\Delta n=\Delta n_c=1/\pi r_e r_0^2$,[2,6] which is independent of wavelength and mode number.

In general, Eqs. (5) and (6) have the form $d^2r_s/dz^2=-\partial V/\partial r_s$, where the effective channel potential $V(r_s)$ is given by $\partial V/\partial r_s=-4/k^2r_s^3-4B/kr_s$. Figure 5 shows the normalized channel potential $\hat{V}(r_s)=(k^2r_0^2/2)V$ vs r_s/r_0 for (a) the fundamental mode with $r_{\rm ch}=3r_0$ (solid curve), $r_{\rm ch}=2r_0$ (dashed curve), and $r_{\rm ch}=r_0$ (dotted curve); and (b) the $r_{\rm ch}=3r_0$ case for the fundamental ($m=p=0$) mode (solid curve), the first order axisymmetric ($m=1$, $p=0$) mode (dashed curve), and the first order nonaxisymmetric ($m=0$, $p=1$) mode (dotted curve), for the parameters $n_0=\Delta n=\Delta n_c$. Trapping of a mode requires $V(r_s)$ to have a local minimum, the position of which defines the matched spot size $r_s=r_{s0}$. A trapped mode will oscillate about r_{s0} with $r_{\rm min}<r_s<r_{\rm max}$, where $r_{\rm max}>r_{s0}$ is the position of the local maximum $V_{\rm max}$ and $r_{\rm min}<r_{s0}$ is the corresponding position at which $V=V_{\rm max}$. The amplitude of the oscillation depends on the initial conditions dr_s/dz and r_s at the channel entrance ($z=0$). Modes are more difficult to trap for increasing m and p and for decreasing $r_{\rm ch}$.

Although the single mode SDE theory neglects leakage, the envelope formulation provides useful information on the initial trapping and distribution of modes within the channel.

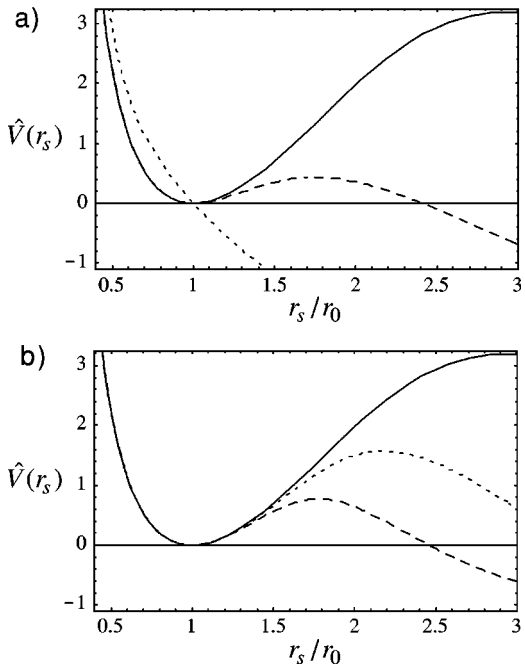

FIG. 5. Normalized channel potential $\hat{V}(r_s)=(k^2r_0^2/2)V$ vs r_s/r_0 for (a) the fundamental mode with $r_{ch}=3r_0$ (solid curve), $r_{ch}=2r_0$ (dashed curve), and $r_{ch}=r_0$ (dotted curve); and (b) the $r_{ch}=3r_0$ case for the fundamental ($m=p=0$) mode (solid curve), the first order axisymmetric ($m=1$, $p=0$) mode (dashed curve), and the first order nonaxisymmetric ($m=0$, $p=1$) mode (dotted curve), for the parameters $n_0=\Delta n=\Delta n_c$.

First of all, a mode can only be trapped in the channel if $V(r_s)$ has a local minimum. Secondly, the bulk of the pulse energy will only be trapped provided $r_{min}<r_{si}<r_{max}$, assuming the entrance conditions $dr_s/dz=0$ and $r_s=r_{si}$. If $r_{si}<r_{min}$ or $r_{si}>r_{max}$, the majority of the pulse energy will not be captured and will diffract from the channel. Hence r_{max} and r_{min} define the acceptance of the channel. Furthermore, if the entrance conditions are such that the mode is not perfectly matched, e.g., $r_{si}\neq r_{s0}$, then the spot size $r_s(z)$ oscillates about r_{s0}. This oscillation is equivalent to exciting several higher-order ''matched spot size'' (MSS) modes, i.e., modes with a constant spot size $r_s=r_{s0}$, as is evident by expanding $\exp(-r^2/r_s^2)$ about $r_s=r_{s0}$ for an oscillation of the form $r_s=r_{s0}+\delta r_0\cos k_\beta z$, where δr_0 is the oscillation amplitude and k_β is the betatron wave number.[33] Hence, depending on the amplitude of the r_s oscillation, which is a function of the entrance conditions, the envelope equation yields the initial distribution of MSS modes excited within the channel. Whether or not these higher-order MSS modes are trapped, and how strongly trapped they are (i.e., the leakage rate), depends on the shape of the effective channel potential V for each of these higher-order modes.

The leakage of a quasibound mode can be estimated with WKB theory as in Sec. III A. The radial mode structure is approximately described by $(\nabla_r^2+K^2)\hat{E}(r)\simeq 0$, with $K^2\simeq\omega^2/c^2-k_p^2(r)-k_z^2-p^2/r^2$ and $k_z^2\simeq\omega^2/c^2-k_{p0}^2-4(2m+p+1)/r_0^2$. In a finite channel, a quasibound mode can exist in the region in which $K^2>0$, i.e., in the region $r_1<r<r_2<r_{ch}$ where $r_{1,2}$ are the turning points given by $K^2=0$. In the region $r_2<r<r_{ch}$, $K^2<0$ and the mode is evanescent.

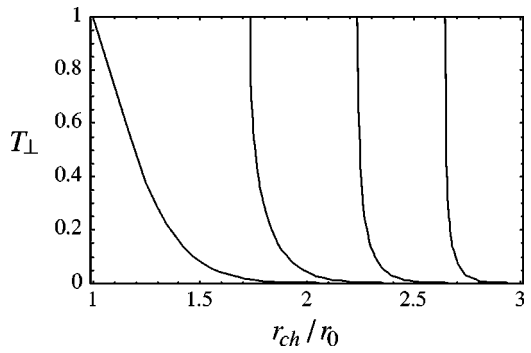

FIG. 6. Tunneling coefficient $T_\perp$ vs r_{ch}/r_0 for the axisymmetric modes $m=0$ (left most curve), $m=1$, $m=2$, and $m=3$ (right most curve) for $\Delta n=\Delta n_0$.

Hence, in a finite channel the mode can tunnel through the region $r_2<r<r_{ch}$ and leak from the channel into the plasma free region $r>r_{ch}$. An approximate requirement for the existence of a quasibound mode is $r_2<r_{ch}$. For a finite parabolic channel, $r_2<r_{ch}$ implies

$$r_{ch}^2>\{(2m+p+1)+[(2m+p+1)^2-p^2]^{1/2}\}r_0^2/2. \quad (7)$$

For the fundamental ($m=p=0$) mode, this implies $r_{ch}>r_0$, where r_0 is defined by $\Delta n=\Delta n_c=1/\pi r_e r_0^2$.

Using WKB tunneling theory,[30] the power leakage of a mode can be described via $P/P_0\simeq\exp(-T_\perp z/Z_p)$, where $T_\perp$ and Z_p are given by Eqs. (2) and (3) with $|K_x|\rightarrow|K|$ and regions of integration $r_2<r<r_{ch}$ and $r_1<r<r_2$, respectively. For axisymmetric modes ($p=0$) in a finite parabolic channel

$$T_\perp=\left[\frac{r_{ch}}{r_2}+\left(\frac{r_{ch}^2}{r_2^2}-1\right)^{1/2}\right]^\beta\exp\left[-2\frac{r_{ch}r_2}{r_0^2}\left(\frac{r_{ch}^2}{r_2^2}-1\right)^{1/2}\right] \quad (8)$$

and $Z_p=\pi k_z r_0^2/2$, where $\beta=2r_2^2/r_0^2$ and $r_2^2=(2m+1)r_0^2$. Note that $Z_p\simeq 2\pi/k_\beta$, where $k_\beta=2/Z_R$ is the betatron wavelength for a mismatch mode[33] and $Z_R=kr_0^2/2$. Equation (8) applies to quasibound modes with $r_2<r_{ch}$. Figure 6 shows the tunneling coefficient $T_\perp$ vs r_{ch}/r_0 for the axisymmetric modes $m=0$ (left most curve), $m=1$, $m=2$, and $m=3$ (right most curve) for $\Delta n=\Delta n_c$. For each mode, $T_\perp=1$ at $r_{ch}=r_2=(2m+1)^{1/2}r_0$. For $r_{ch}<r_2$, the modes diffract from the channel at nearly the vacuum rate. For $r_{ch}>r_2$, the modes leak from the channel at a reduced rate, i.e., $dP_{ch}/dz\sim(T_\perp/\pi Z_R)P_{ch}$, where P_{ch} is the mode power confined within the channel.

IV. GUIDING

This section describes experimental results on guiding high intensity laser pulses in the 1D slab plasma channel geometry. The laser pulse (injection pulse) was focused near the entrance of the channel using an off-axis parabola. The time delay between the ignitor pulse and the injection pulse was fixed to 600 ps. (This constraint arose from physical limitations in the available vacuum chamber.)

To diagnose the guiding, the laser beam was imaged onto a charged-coupled device (CCD) camera using a 1 in.

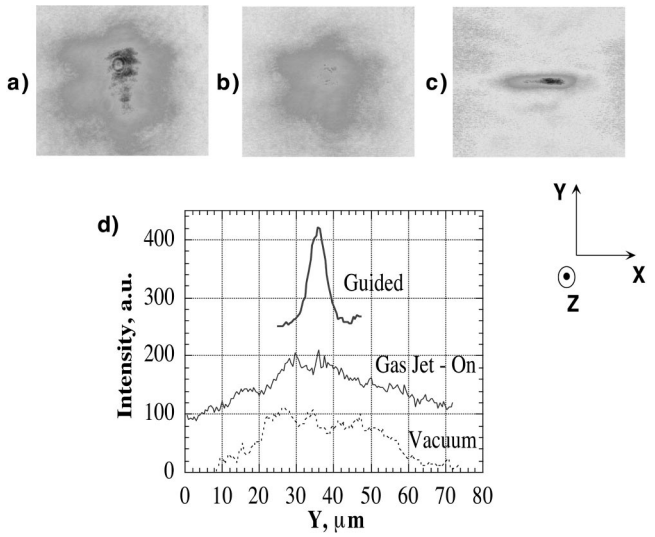

FIG. 7. Transverse laser beam images, slab channel geometry: (a) gas jet turned off, (b) gas jet on, without heater pulse, and (c) guided by the channel, gas jet backed with nitrogen at 1000 psi, and (d) the corresponding vertical line outs.

diam MgF_2 lens of focal length $f_l = 68.3$ mm at 800 nm. The CCD camera was mounted on an optical rail allowing a change in position of the object plane with a range of 50 cm. The resolution and magnification of the imaging system was calibrated for different CCD camera locations.

Figure 7 shows images of the injection laser pulse (75 fs, 20–40 mJ, with a minimum focal spot size of ~ 5 μm in vacuum, i.e., $\sim 5\times 10^{17}$ W/cm^2) for (a) propagating through vacuum (gas jet turned off), (b) after undergoing ionization induced refraction[25] in the gas jet plume without the heater pulse being present, hence no channel formed, and (c) guided by the channel, for a gas jet backed with nitrogen at 1000 psi. Vertical line outs of these images, shown in Fig. 7(d), clearly demonstrate the changes induced by the plasma channel on the guided laser pulse. The guided spot size near the end of the channel was $\sim 8\,\mu\text{m}\times 50\,\mu$m. The reduction in vertical beam size by ~eight times provided by the channel is consistent with a laser beam of $Z_R \sim 0.1$ mm propagating a distance of ~0.8 mm (the half-width of the jet).

As seen in Fig. 2, for the in-plane ignitor and heater pulse configuration, plasma channels were created in an elongated, elliptical shape. In turn, the guided beam images [Fig. 7(c)] had a similar elongated shape.

As the gas jet was moved further away from the laser focus, larger portions of the injected laser energy did not couple into the channel. To obtain a quantitative measurement for the guiding properties of these channels, the image intensity integral of the CCD images was used as a measure of the laser energy. This allowed a comparison of the amount of the laser energy guided by the channel to the total intensity integral of the CCD image (full beam energy, E_{full}). The intensity integral of the isolated central lobe of the images was taken to be the guided energy.

The ratio of the guided energy, E_g, to the total image intensity integral, E_{full} is shown in Fig. 8. As expected, the fraction of the laser beam that is coupled into the channel

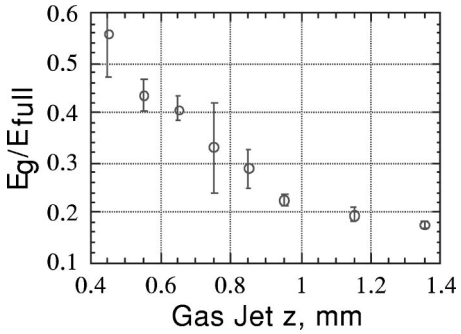

FIG. 8. Ratio of energy in the guided central lobe, E_g, to that of the full beam, E_{full}, plotted vs the gas jet position, z, where $z=0$ corresponds to the injection pulse focus being in the center of the gas jet plume (half-width of the gas jet plume is ~0.8–1 mm).

becomes larger as the injection pulse focus is moved closer to the jet's edge than when the gas jet is moved further away from the laser focus position in vacuum. It should be noted that the F numbers of the off-axis parabola and the imaging MgF_2 lens are rather close and the collection angle is limited. Nevertheless, the leakage of the fundamental mode of the plasma channel is fully collected.

As the laser waist is moved closer to the channel entrance, the laser spot size becomes comparable with the channel size and most of the power is coupled to the modes of the channel. The ratio of E_g to the E_{full} approaches ~55%. This number is in good agreement with previous analytical results (Sec. III A), where the leakage fraction was estimated to be ~50%.

To demonstrate the dependence of the number of guided modes on the channel depth, shadowgrams of the round channels (90° geometry in H_2) were taken with variable time delay with respect to the arrival time of the heater pulse. As the shock wave propagates further out, leaving a deeper plasma density depression on the channel axis, the guided part of the probe beam couples to higher and higher-order modes of the channel. Figure 9 presents the results of such a time delay scan taken with a channel created in hydrogen. The increase in the number of lobes in the guided part of the blue pulse for longer probe pulse delays demonstrates the dependence of the number of guided modes on the channel depth and width. Similar measurements were previously reported for channels created in high Z gases.[8,9]

Guiding of intense pulses is currently being evaluated using these round channels. In the case of slab-like channels, the injected intensity was $\sim 5\times 10^{17}$ W/cm^2 and the intensity at the channel exit was $\sim 1\times 10^{16}$ W/cm^2. This reduction in intensity was due to only 20% transmission efficiency (due to mode mismatch and leakage losses) and due to the fact that guiding was primarily occurring in only 1D. The use of cylindrically symmetric channels will provide guiding in both dimensions and, with proper mode matching, guided intensities on the order of $\sim 5-10\times 10^{17}$ W/cm^2 are expected.

V. TIME DOMAIN REFRACTOMETRY WITH HOLOGRAPHIC INVERSION

To perform phase shift measurements which are precise and insensitive to noise and fluctuations, a Rayleigh inter-

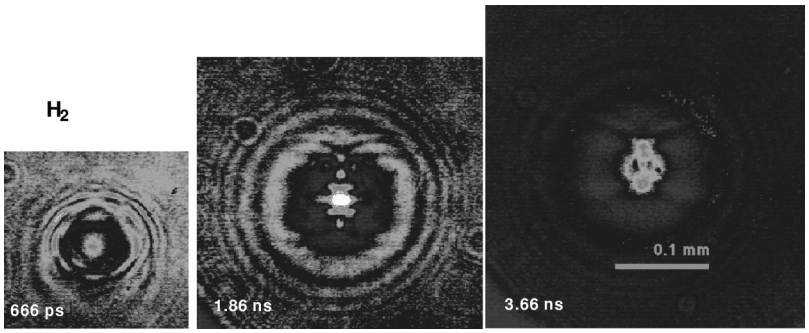

FIG. 9. Shadowgrams of round channels created in hydrogen at three different time delays after the heating: 666 ps (left), 1.86 ns (center), and 3.66 ns (right).

ferometric refractometer technique was applied successfully[28,29] to measure phase shifts on the order of several mrads. This technique utilizes two laser pulses, propagating down the same path, but separated by a time delay. The leading of the two pulses traverses the plasma before the intense pulse that drives the plasma wake. The trailing pulse propagates through the plasma after the wake was produced. Thus the difference in the phase shift acquired by the two laser pulses is due to the plasma wave. The interferometric pulses are subsequently combined in an imaging grating spectrometer. After diffracting off the grating the obtained pattern is viewed by a CCD camera at the image plane. Because of the pulse stretching caused by the diffraction grating, the two laser pulses now overlap in time and a beat pattern is seen on the CCD. By simply Fourier transforming this beat pattern, the phase shift can be retrieved. However, this direct method provides the correct phase shift information only in the case when the phase shift is constant in time. Following a brief mathematical description of the standard Fourier domain interferometry technique, a further generalization based on holographic-type inversion is presented, that enables retrieval of more complicated phase shift beyond the capabilities of the standard method.

The spatial periodicity of the beat pattern is directly related to the time separation between the two pulses. The temporal stretching T_s in a spectrometer can be calculated if the resolution of the spectrometer R_s is known: $T_s \sim 1/R_s$, e.g., a resolution of $\delta\lambda = 0.114\,\mathrm{nm}$ translates into pulse lengthening of $T_s \sim (\omega \delta\lambda/\lambda)^{-1} = 3\,\mathrm{ps}$ for 800 nm radiation. As an example, assume that the electric field of two laser pulses incident at the entrance slit of a grating spectrometer is of the form $E(t) = \exp[-(t+\Delta t)^2/\tau^2]\cos[\omega_0(t+\Delta t)] + \exp(-t^2/\tau^2)\cos(\omega_0 t + \phi)$, where ω_0 is the central laser frequency, τ is the pulse duration, Δt is the time delay, and ϕ is the phase shift acquired from the plasma. The action of the (perfect) grating spectrometer is equivalent to taking one half of the Fourier transform of the pulses (positive or negative frequency): $F(\omega) = (\sqrt{\pi}/2)\tau \exp(-\delta\omega^2\tau^2/4)[\exp(-i\delta\omega\Delta t) + \exp(-i\phi)]$, where $\delta\omega = \omega - \omega_0$. A CCD camera measures time integrated power (proportional to the absolute value of the electric filed squared). The measured pattern will contain contributions from dc terms of the individual pulse amplitudes and the beating cross term with frequency domain variation as $\cos(\phi + \delta\omega\Delta t)$

$$P(\omega) \propto 2\exp(-\delta\omega^2\tau^2/2) + 2\exp(-\delta\omega^2\tau^2/4) \times \cos(\phi + \delta\omega\Delta t). \tag{9}$$

The interference pattern shifts in the spectral domain if the probe pulse has acquired a phase shift with respect to the reference pulse. A constant phase shift, ϕ, can be extracted from the beating pattern by performing a Fourier transform of the spectrum with respect to $\delta\omega$.

As mentioned previously, a simple Fourier transformation of the spectral beat provides correct phase shift information only in the case when the phase shift is constant in time. For instance, in the case of a linearly changing (in time) phase shift, the retrieved phase has a slope that is two times smaller than the actual.[28] The reason for the discrepancy is that instead of taking an inverse Fourier transform of the Fourier transform of the probe pulse, the diagnostic calculates the inverse Fourier transform of the product of the probe and reference pulse transforms. If the amplitude of the Fourier transform of the reference pulse is known, and if the only phase difference between the probe and reference pulses is due to the plasma wake (so that any other phase shift that is common to both pulses will cancel when a product with complex conjugate is taken), then by dividing the spectral beat by the amplitude of the reference pulse Fourier transform (square root of the spectrum of the reference pulse alone) before the Fourier transformation is calculated, the true phase shift is found. This procedure is similar to the action of the reference pulse in a hologram.

Figure 10 presents a numerical simulation of the phase shift retrieval with and without the holographic correction. The result of numerically calculating the inverse Fourier transform of Eq. (9) with $\phi = \phi_{\max}\cos(\omega_p t + \Phi_0)$, where $\phi_{\max} = 182\,\mathrm{mrad}$ is expected to be close to the experimental values, is shown in Fig. 10(a). Figure 10(b) presents the result of taking the Fourier transform after the expression of Eq. (9) was corrected for the reference pulse Fourier transform amplitude. The phase shift retrieved without the holographic correction, Fig. 10(a), is drastically different from the actual phase shift. The corrected retrieval, Fig. 10(b), is shown to extract the prescribed time dependent phase shift accurately.

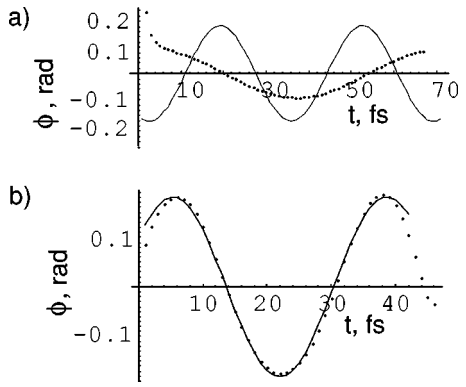

FIG. 10. Retrieved phase shift (dots) (a) without and (b) with reference correction, compared to that prescribed (solid curves).

VI. CONCLUSIONS

To overcome the laser diffraction length limit, a novel method of plasma channel production for laser guiding, the ignitor-heater technique, was proposed and tested experimentally. With this technique, plasma channels can be created in hydrogen and deeply ionized nitrogen without high atomic number additives, thereby allowing high intensity laser pulse guiding. To avoid ionization induced refraction of the guided laser pulse, channels were formed in a plume of a pulsed gas jet. It should also be noted that the ignitor-heater scheme employs cylindrical optics that are out of the path of the accelerator beam (for plasma-based accelerator applications) and, potentially, allows the recycling of the laser beams. The channel formation process was fully characterized with time resolved two-dimensional (2D) longitudinal interferometry diagnostic using a sub-ps probe pulse. The shape of the initial spark was proven to affect the shape of the plasma channel. By using in-plane or orthogonal beam combining configurations, elongated, or slab channels, with 1D guiding properties and cylindrically symmetric, round, channels with guiding in both transverse dimensions were created in both nitrogen and hydrogen.

Laser pulses at high intensity ($\sim 5\times 10^{17}\,\mathrm{W/cm^2}$) were injected in nitrogen slab channels and observed to be guided over $\sim$5–10 Rayleigh lengths, limited by the gas jet length. Leakage and transmission measurements were found to agree well with the theoretical predictions. Due to the fact that guiding only occurred in 1D and that mode matching resulted in poor coupling, guided intensities at the exit of the channel were on the order of $\sim 1-5\times 10^{16}\,\mathrm{W/cm^2}$. The use of cylindrically symmetric channels is expected to increase the guiding efficiency and, with proper mode matching and higher laser power, guided intensities $>5\times 10^{17}\,\mathrm{W/cm^2}$ are expected.

Single mode and multimode laser propagation in round channels was observed as a function of time delay of the probe pulse injection after the spark heating. The modal content is found to be in good qualitative agreement with the predictions of the leakage theory in 2D.

An analytic theory was developed to describe laser pulse propagation in parabolic channels of finite transverse extent. Using the SDE method, an envelope equation was derived to describe the evolution of the laser spot size for an arbitrary Laguerre–Gaussian mode in the channel. For a given channel profile, the envelope equation describes under what initial conditions (spot size and convergence angle at the channel entrance) the bulk of the laser energy will be trapped within the channel. If the laser pulse is not perfectly matched in the channel, its spot size oscillates about the matched value, which is equivalent to exciting higher-order modes. Hence, the envelope equation enables one to calculate the modal distribution of the laser energy initially excited within the channel. Once this is known, the leakage of energy (tunneling through the channel wall) for a given mode can be calculated with a WKB method.

In addition, a holographic-type correction to the longitudinal fs interferometry diagnostic was proposed and numerically simulated. This enables accurate retrieval of the time varying phase shift, providing an optical based method for measuring time-varying wake fields in plasma-based acceleration experiments.

ACKNOWLEDGMENTS

The authors acknowledge useful conversations with P. Catravas, C. B. Schroeder, B. A. Shadwick, and J. S. Wurtele. This work was supported by the U.S. Department of Energy under contract No. DE-AC-03-76SF0098.

[1]For a review see, E. Esarey, P. Sprangle, J. Krall, and A. Ting, IEEE J. Quantum Electron **33**, 1879 (1997).
[2]T. Tajima and J. M. Dawson, Phys. Rev. Lett. **43**, 267 (1979); For a review see, E. Esarey, P. Sprangle, J. Krall, and A. Ting, IEEE Trans. Plasma Sci. **24**, 252 (1996); W. P. Leemans, C. W. Siders, E. Esarey, N. Andreev, G. Shvets, and W. B. Mori, *ibid.* **24**, 331 (1996).
[3]H. M. Milchberg, C. G. Durfee III, and T. J. MacIlrath, Phys. Rev. Lett. **75**, 2494 (1995); C. G. Durfee, S. Backus, M. M. Murnane, and H. C. Kapteyn, Opt. Lett. **22**, 1565 (1997).
[4]N. H. Burnett and P. B. Corkum, J. Opt. Soc. Am. B **6**, 1195 (1989); D. C. Eder, P. Amendt, L. B. DaSilva *et al.*, Phys. Plasmas **1**, 1744 (1994); S. Suckewer and C. H. Skinner, Comments At. Mol. Phys. **30**, 331 (1995).
[5]M. Tabak, J. Hammer, and M. E. Glinsjy *et al.*, Phys. Plasmas **1**, 1626 (1994); A. Pukhov and J. Meyerter-Vehn, Phys. Plasmas **5**, 1880 (1998).
[6]P. Sprangle and E. Esarey, Phys. Fluids B **4**, 2241 (1992); P. Sprangle, E. Esarey, J. Krall, and G. Joyce, Phys. Rev. Lett. **69**, 2200 (1992).
[7]L. C. Johnson and T. K. Chu, Phys. Rev. Lett. **32**, 517 (1974).
[8]C. G. Durfee III, and H. M. Milchberg, Phys. Rev. Lett. **71**, 2409 (1993); C. G. Durfee III, J. Lynch, and H. M. Milchberg, Opt. Lett. **19**, 1937 (1994); C. G. Durfee III, J. Lynch, and H. M. Milchberg, Phys. Rev. E **51**, 2368 (1995); H. M. Milchberg, T. R. Clark, C. G. Durfee, T. M. Antonsen, and P. Mora, Phys. Plasmas **3**, 2149 (1996); S. P. Nikitin, T. M. Antonsen, T. R. Clark, Y. L. Li, and H. M. Milchberg, Opt. Lett. **22**, 1787 (1997).
[9]T. R. Clark and H. M. Milchberg, Phys. Rev. Lett. **78**, 2373 (1997); **81**, 357 (1998).
[10]V. Malka, E. de Wispelaere, F. Amiranoff *et al.*, Phys. Rev. Lett. **79**, 2979 (1997).
[11]T. Ditmire, R. A. Smith, and M. H. R. Hutchinson, Opt. Lett. **23**, 322 (1998).
[12]W. P. Leemans, P. Volfbeyn, K. Z. Guo *et al.*, Phys. Plasmas **5**, 1615 (1998).
[13]P. Volfbeyn and W. P. Leemans, in *Proceedings of the 6th European Particle Accelerator Conference*, edited by S. Myers, L. Liljeby, Ch. Petit-Jean-Genaz, J. Poole, and K. G. Rensfelt (Inst. of Phys., Philadelphia, 1998), p. 265; P. Volfbeyn, Ph.D. thesis, MIT, LBNL Report No. 41892 (1998).
[14]E. Gaul, S. P. Le Blanc, and M. C. Downer, *Advanced Accelerator Concepts*, edited by W. Lawson, AIP Conf. Proc. (American Institute of Physics, Woodbury, NY, 1999).
[15]Y. Ehrlich, C. Cohen, A. Zigler, J. Krall, P. Sprangle, and E. Esarey, Phys. Rev. Lett. **77**, 4186 (1996); Y. Ehrlich, C. Cohen, D. Kaganovich, A.

Zigler, R. F. Hubbard, P. Sprangle, and E. Esarey, J. Opt. Soc. Am. B **15**, 2416 (1998).
[16]K. Krushelnick, A. Ting, C. I. Moore, H. R. Burris, E. Esarey, P. Sprangle, and M. Baine, Phys. Rev. Lett. **78**, 4047 (1997); A. Ting, C. I. Moore, K. Krushelnick *et al.*, Phys. Plasmas **4**, 1889 (1997).
[17]S. Y. Chen, G. S. Sarkisov, A. Maksimchuk, R. Wagner, and D. Umstadter, Phys. Rev. Lett. **80**, 2610 (1998).
[18]A. B. Borisov, X. Shi, V. B. Karpov *et al.*, J. Opt. Soc. Am. B **11**, 1941 (1994).
[19]P. Gibbon, F. Jakober, P. Monet, and T. Auguste, IEEE Trans. Plasma Sci. **24**, 343 (1996).
[20]A. Chiron, G. Bonnaud, A. Dulieu, J. L. Miquel, G. Malka, and M. Louis-Jacquet, Phys. Plasmas **3**, 1373 (1996).
[21]P. E. Young and P. R. Bolton, Phys. Rev. Lett. **77**, 4556 (1996).
[22]M. Borghesi, A. J. MacKinnon, L. Barringer *et al.*, Phys. Rev. Lett. **78**, 879 (1997).
[23]J. Fuchs, G. Malka, J. C. Adam *et al.*, Phys. Rev. Lett. **80**, 1658 (1998).
[24]C. E. Clayton, K. C. Tzeng, D. Gordon *et al.*, Phys. Rev. Lett. **81**, 100 (1998).
[25]W. P. Leemans, C. E. Clayton, W. B. Mori *et al.*, Phys. Rev. A **46**, 1091 (1992); W. P. Leemans, C. E. Clayton, W. B. Mori *et al.*, Phys. Rev. Lett. **68**, 321 (1992).
[26]S. Augst, D. Strickland, D. D. Meyerhofer, S. L. Chin, and J. H. Eberly, Phys. Rev. Lett. **63**, 2212 (1989).
[27]C. D. Decker, W. B. Mori, J. M. Dawson, and T. Katsouleas, Phys. Plasmas **1**, 4043 (1994); G. Shvets and N. J. Fisch, *ibid.* **4**, 428 (1997).
[28]C. W. Siders, S. P. Le Blanc, D. Fisher *et al.*, Phys. Rev. Lett. **76**, 3570 (1996).
[29]J. R. Marques, J. P. Geindre, F. Amiranoff, P. Audebert, J. C. Gauthier, A. Antonetti, and G. Grillon, Phys. Rev. Lett. **76**, 3566 (1996).
[30]A. W. Snyder and J. D. Love, *Optical Waveguide Theory* (Chapman and Hall, New York, 1983).
[31]P. Sprangle, J. Krall, and E. Esarey, Phys. Rev. Lett. **73**, 3544 (1994).
[32]E. Esarey, J. Krall, and P. Sprangle, Phys. Rev. Lett. **72**, 2887 (1994).
[33]E. Esarey and W. P. Leemans, Phys. Rev. E **59**, 1082 (1999).